

StePS: A Multi-GPU Cosmological N-body Code for Compactified Simulations

Gábor Rácz^a, István Szapudi^b, László Dobos^a, István Csabai^a, Alexander S. Szalay^c

^a*Department of Physics of Complex Systems, Eötvös Loránd University, Pf. 32, H-1518 Budapest, Hungary*

^b*Institute for Astronomy, University of Hawai‘i, 2680 Woodlawn Drive, Honolulu, HI, 96822*

^c*Department of Physics and Astronomy and Department of Computer Science, Johns Hopkins University, 3400 N. Charles Street, Baltimore, MD 21218*

Abstract

We present the multi-GPU realization of the StePS (Stereographically Projected Cosmological Simulations) algorithm with MPI-OpenMP-CUDA hybrid parallelization, and show what parallelization efficiency can be reached. We use a new zoom-in cosmological direct N-body simulation method, that can simulate the infinite universe with unprecedented dynamic range for a given amount of memory and, in contrast to traditional periodic simulations, its fundamental geometry and topology match observations. By using a spherical geometry instead of periodic boundary conditions, and gradually decreasing the mass resolution with radius, our code is capable of running simulations with a few gigaparsecs in diameter and with a mass resolution of $\sim 10^9 M_\odot$ in the center in four days on three compute nodes with four GTX 1080 Ti GPUs each. The code can also be used to run extremely fast simulations with reasonable resolution for fitting cosmological parameters. These simulations can be used for prediction needs of large surveys. The **StePS** code is publicly available for the research community.

Keywords: methods: numerical, methods: N-body simulations, GPU, cosmology: dark matter, cosmology: large-scale structure of universe

1. Introduction

Cosmological N-body simulations are playing an important role in understanding the structure formation of the dark matter in the non-linear regime. With these simulations the $P(k)$ power spectrum, the $Cl(r)$ spherical power spectrum, and the halo mass function can be calculated for testing the cosmological models and for fitting cosmological parameters. In a last 44 years these simulations went through a great improvements: from the first simulations that had only 10^3 particles[1], nowadays it is possible to run a simulation with 8 trillion dark matter particles[2]. This speed up achieved by faster computers and by algorithmic improvements with the use of tree-algorithms and Fourier transformation methods.

Most of these simulations are running in a finite cubic volume with periodic boundary condition which is not supported by the observations, and causes distortions in the gravitational force field. Our **StePS** algorithm eliminates the need for these artificial boundaries, and can simulate an infinite Universe with a topology that matches the observations[3]. This approach can achieve unprecedented dynamic range with the use of small number of particles, using a unique isotropic zoom-in method involving the compactification of the spatial extent of the Universe. The relatively small number of particles makes possible the use of direct force summation with low memory needs. This approach is ideal for a relatively simple and very effective GPU parallelization.

We demonstrated the effectiveness of this method in our previous paper[3]. The structure of this paper is the following: we present the detailed simulation algorithm with a new multi-GPU parallelization in Section 2. In Section 3 we show how

one can generate initial conditions for the **StePS** simulation code. Section 4 describes the example simulations that we run to demonstrate the parallelization effectiveness of our code.

2. The simulation algorithm

2.1. Compactified cosmological simulations

It is impossible to simulate the infinite universe with constant resolution in a computer with finite memory and processing power. The traditional cosmological simulations solve this problem by using periodic boundary conditions. This essentially means that the infinite universe is tiled by exactly identical cubic volumes that are repeated in an infinite simple cubic grid. These simulations have translation-symmetry, but they lack rotational symmetry because of the characteristic directions of the grid. This is not the only way to run a cosmological simulation. The **StePS** algorithm is built on the idea, that an infinite universe can be represented in a finite volume using compactification. Compactifying the space around a chosen point in radial direction and choosing a constant resolution in the compact space leads to an isotropic geometry that have the rotational symmetry but lacks the translation-symmetry. In this case, the decompactified real space has a constant angular and continuously decreasing radial resolution in radial direction, thus this simulation is a specific zoom-in simulation. The calculation of the force field is more complicated in the compact space than in the real space in Cartesian coordinates, hence it would require more computations. Therefore, we transform back the constant resolution compact space into the real space, to make the simulations significantly faster.

The last cell in radial direction corresponds to an infinite volume in the real space, so it needs a special treatment. Because this is an infinite homogeneous volume, the effect of this region can be calculated analytically, and it yields a simple radial force depending only on the average density.

The original **StePS** algorithm uses the inverse 3 dimensional stereographic projection and remapped in the compact space. These are transformations between a three-dimensional hypersurface of the four dimensional hypersphere and the three-dimensional "real" space. If Cartesian coordinates are used in the three-dimensional space, the transformation rules for the inverse stereographic projection becomes

$$\begin{aligned}\omega &= 2 \cdot \arctan \left(\frac{\sqrt{x^2 + y^2 + z^2}}{D_s} \right) \\ \vartheta &= \cos^{-1} \left(\frac{z}{\sqrt{x^2 + y^2 + z^2}} \right) \\ \varphi &= \arctan \left(\frac{y}{x} \right)\end{aligned}\quad (1)$$

where ω , ϑ and φ are the coordinates on the three-dimensional hypersurface of the four dimensional hypersphere, D_s is the diameter of the sphere, and x , y , z are the coordinates in the real space. The

$$\begin{aligned}x &= D_s \cdot \tan \left(\frac{\omega}{2} \right) \sin(\vartheta) \cos(\varphi) \\ y &= D_s \cdot \tan \left(\frac{\omega}{2} \right) \sin(\vartheta) \sin(\varphi), \\ z &= D_s \cdot \tan \left(\frac{\omega}{2} \right) \cos(\vartheta)\end{aligned}\quad (2)$$

stereographic projection is used to transform back the compactified hypersurface into the real space. These transformations are only used when the initial condition is generated. The **StePS** code can be used with any initial condition that was made with isotropic compactification map (e.g. only radial compactification was done).

2.2. Basic Equations

The expansion of the Universe governed by the Friedmann equations. The first equation can be written as

$$\left(\frac{\dot{a}}{a} \right)^2 = H_0^2 \cdot (\Omega_m \cdot a^{-3} + \Omega_r \cdot a^{-4} + \Omega_\Lambda + \Omega_k \cdot a^{-2}), \quad (3)$$

where $a(t)$ is the scale factor, H_0 is the Hubble constant, and $H = \dot{a}/a$ is the Hubble-parameter. The Ω density parameters are defined by the ratio of the component energy-density to the critical density. Here we use the present day values. The density parameters are the following: Ω_m is the non-relativistic matter density parameter, Ω_Λ is the dark energy density, Ω_r is the radiation energy-density and Ω_k is the spatial curvature density. This equation is used for each type of cosmological simulations in the **StePS** code.

The evolution of the dark matter structures in an expanding universe are usually solved by the N-body method[4]. In this approximation the dark matter continuum is sampled by a

finite number of tracer particles. There is only gravitational interaction between these dark-matter particles. Our code can run traditional periodic, and compactified spherical simulations. Below, we describe the basic equations for both simulation method.

2.2.1. Traditional Periodic Simulations

The equations of motion in the Newtonian approximation, in comoving coordinate system are

$$m_i \ddot{\mathbf{x}}_i = \sum_{j=1; j \neq i}^N \frac{m_i m_j \mathbf{F}(\mathbf{x}_i - \mathbf{x}_j, h_i + h_j)}{a(t)^3} - 2 \cdot m_i \cdot \frac{\dot{a}(t)}{a(t)} \cdot \dot{\mathbf{x}}_i, \quad (4)$$

where \mathbf{x}_i and m_i are the comoving coordinates and the masses of the particles, h_i and h_j are the softening lengths of the associated particles. The function $m_i m_j \mathbf{F}(\mathbf{x}_i - \mathbf{x}_j, h_i + h_j)$ is magnitude of the force between the i and j particle, and it depends on the boundary conditions and on the softening kernel. The **StePS** code uses the spline kernel[4, 5] for gravitational softening. For zero boundary conditions, the $\mathbf{F}(\mathbf{x}, h)$ is given by

$$\mathbf{F}(\mathbf{x}, h) = -G \mathcal{F}(|\mathbf{x}|, h) \frac{\mathbf{x}}{|\mathbf{x}|} \quad (5)$$

where G is the gravitational constant, and

$$\mathcal{F}(r, h) = \begin{cases} \frac{32r^4}{h^6} - \frac{38.4r^3}{h^5} + \frac{32r}{3h^3} & \text{if } r < \frac{h}{2} \\ -\frac{32r^4}{3h^6} + \frac{38.4r^3}{h^5} - \frac{48r^2}{h^4} + \frac{64r}{3h^3} - \frac{1}{15r^2} & \text{if } \frac{h}{2} < r < h \\ \frac{1}{r^2} & \text{if } h < r \end{cases}. \quad (6)$$

The softening length is set at the beginning of the simulation, and for a constant spatial resolution case, it is the same for every particle.

For this periodic case, multiple images of the particles are taken into account with the

$$\mathbf{F}(\mathbf{x}, h) = \sum_{\mathbf{n}} -G \mathcal{F}(|\mathbf{x} - \mathbf{n}L|, h) \frac{\mathbf{x} - \mathbf{n}L}{|\mathbf{x} - \mathbf{n}L|} \quad (7)$$

Ewald summation[6, 7], where L is the linear size of the periodic box, and $\mathbf{n} = (n_1, n_2, n_3)$ extends over all integer triplets, in theory up to infinity. A numerical code can not sum for all integer triplets, so a cut in \mathbf{n} is required. Our code is using the following cut in \mathbf{n} : the only valid triplets are where $|\mathbf{x} - \mathbf{n}L| < 2.6L$ is fulfilled[7]. It is also possible to use quasi-periodic boundary conditions: in this case, only the largest element of the eq. 7 sum will be used for each pair of particles. If the simulation has constant resolution everywhere in the periodic box, then the m_i particle masses are calculated directly from the cosmological parameters. In a constant resolution case

$$m_i = \frac{\rho_{crit} \cdot \Omega_m \cdot V_{sim}}{N} = \frac{3 \cdot H_0^2 \cdot \Omega_m}{8\pi G} \cdot \frac{V_{sim}}{N}, \quad (8)$$

is equal for all particle, where V_{sim} is the simulation volume, and N is the number of the particles in the simulation.

2.2.2. Spherical Simulations

In the spherical zoom-in simulations, the average particle separation and the masses of the particles are increasing outwards, so the outer particles represent larger volumes with lower spatial resolution, so eq. 8 can not be used for calculating the masses but we should keep the assumption that at the largest scales the universe is homogeneous, and the total mass of the particles are consistent with the cosmological parameters. The details of particle mass calculation and initial condition generation will be described in section 3 below. For the spherical geometry, we only set the h_{min} softening length for smallest-mass particle, and for the rest of the particles the code calculates

$$h_i = \sqrt[3]{\frac{m_i}{m_{min}}} \cdot h_{min}, \quad (9)$$

where m_{min} is the mass of the smallest-mass particle. With this formula, the average density inside h_i radius around every particle will be the same. The equations of motion in comoving coordinates with non-periodic and isotropic boundary conditions are

$$\ddot{\mathbf{x}}_i = \sum_{j=1; j \neq i}^N \frac{m_j \mathbf{F}(\mathbf{x}_i - \mathbf{x}_j, h_i + h_j)}{a(t)^3} - 2 \cdot \frac{\dot{a}(t)}{a(t)} \cdot \dot{\mathbf{x}}_i + \frac{4\pi G}{3} \bar{\rho} \mathbf{x}_i, \quad (10)$$

where $\mathbf{F}(\mathbf{x}, h)$ is calculated with the spline kernel by using Eq. 5, and $\bar{\rho} = \rho_{crit} \cdot \Omega_m$ is the average matter density. The last part of the right side of the equation is the force coming from the last, infinite radial cell, and it can be derived from Newton's shell theorem[3].

The **StePS** code also can run cosmological simulations with static, non-comoving coordinates in a fully Newtonian way. In order to run these types of simulations, the initial condition in comoving coordinates should be converted to static coordinates with the following transformations:

$$\mathbf{X}_i = a \mathbf{x}_i \quad (11)$$

$$\dot{\mathbf{X}}_i = \frac{\dot{a}}{a} \cdot \mathbf{X}_i + \dot{\mathbf{x}}_i, \quad (12)$$

where \mathbf{x}_i are the comoving, and \mathbf{X}_i are the static coordinates, whereas a is the time dependent scale factor taken at the time of the initial conditions. The equations of motion in this case are

$$m_i \ddot{\mathbf{X}}_i = \sum_{j=1; j \neq i}^N m_i m_j \mathbf{F}(\mathbf{X}_i - \mathbf{X}_j, h_i + h_j) + H_0^2 \Omega_\Lambda \cdot m_i \cdot \mathbf{X}_i. \quad (13)$$

For more detailed discussion, and for deriving these equations, see our previous paper[3].

2.3. Time integration

The most time-consuming part of integrating an N-body system is the calculation of the forces, especially if the forces are calculated directly. It is vital to minimize the number of force calculations per timestep if N is large. For integrating the equations of motion, we used the KDK leapfrog integrator[8]. This is a second order method, yet it needs only one gravitational

force evaluation per timestep. The integrator uses two different operators: the

$$K_i(\Delta t) : \begin{cases} \mathbf{x}_i \longmapsto \mathbf{x}_i \\ \mathbf{v}_i \longmapsto \mathbf{v}_i + \mathbf{A}_i \cdot \Delta t \end{cases} \quad (14)$$

'kick' and the

$$D_i(\Delta t) : \begin{cases} \mathbf{x}_i \longmapsto \mathbf{x}_i + \mathbf{v}_i \cdot \Delta t \\ \mathbf{v}_i \longmapsto \mathbf{v}_i \end{cases} \quad (15)$$

'drift' operator, where \mathbf{A}_i is the acceleration of the particle. The KDK integrator uses two 'kick' and one 'drift' operation per timestep, so the time evolution operator is:

$$\tilde{U}(\Delta t) = K \left(\frac{\Delta t}{2} \right) D(\Delta t) K \left(\frac{\Delta t}{2} \right). \quad (16)$$

The code use adaptive timestep with the KDK integrator. For a constant resolution simulation we adopted the

$$\Delta t = \min \left[\Delta t_{max}, \sqrt{\frac{2\eta_i \epsilon}{|\mathbf{A}_i|}} \right] \quad (17)$$

time-step criterion, where $\eta_i = 2.8 \cdot h_i$ is the Plummer equivalent softening length, ϵ is the accuracy parameter, and $|\mathbf{A}_i|$ is the acceleration of the particle. Δt_{max} is the maximal allowed length for a time-step. The same formula is used in the cosmological code GADGET-2[4].

Most of the cosmological N-body codes are not using different variables for the cosmic time (t) and for the scale factor (a). Instead, the scale factor is used as time-variable, and when the particle positions are updated, the

$$\Delta t = \left(a \cdot H_0 \cdot \sqrt{(\Omega_m \cdot a^{-3} + \Omega_r \cdot a^{-4} + \Omega_\Lambda + \Omega_k \cdot a^{-2})} \right)^{-1} \cdot \Delta a \quad (18)$$

formula is used to calculate the physical time. This can be seen as a first-order Euler integration of the eq. 3 Friedmann-equation. To achieve higher precision, we used the t physical time for the time variable and for cosmological simulations the code integrates the eq. 3 equation with the fourth-order Runge-Kutta method with the same timestep length that the N-body integrator uses.

2.4. Force calculation and parallelization methods

The most time-consuming part of a direct N-body code is the gravitational force calculation, because the execution time scales with N^2 . Every other part of our code scales with N or better, so it is enough to parallelize this part of the program. The **StePS** approach makes possible massively parallel implementation, that is able to run on a large CPU or GPU cluster.

The use of direct force calculation is feasible because compared to the traditional approach the projected simulations have relatively small number of particles with high resolution at the center even for extremely large simulation volumes. The small number of the particles carries another advantage: only

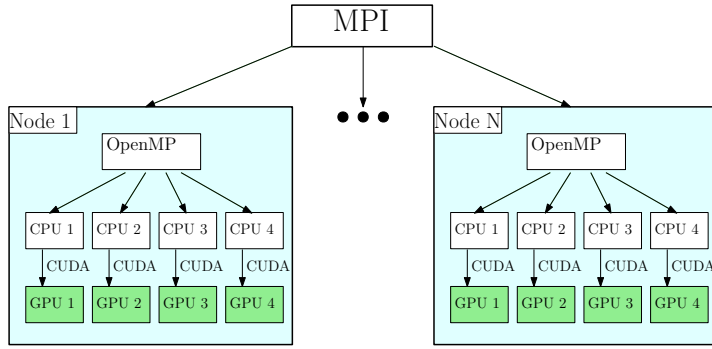


Figure 1: Force calculation in a GPU cluster with MPI-OpenMP-CUDA hybrid parallelization.

a few hundred MBs of memory needed to store all the particle data. Modern GPUs are ideal candidates for this type of calculation: they are ~ 100 times faster than the same priced CPUs, and they have enough memory to store all the particles' data.

For the force calculation, the code have two or three distinct levels of parallelization. The first level is the communication between the nodes in the computing cluster. For this, we used the Open Message Passing Interface¹ (OpenMPI) library. This is an open-source Message Passing Interface implementation. In this level of the force calculation, the "main" node broadcasts the particle coordinates and masses to every other nodes. After the successful force calculation, it collects the calculated forces from every node, to do every other calculation. In the second level, the program uses the Open Multi-Processing² (OpenMP) library for shared-memory force calculation in the nodes. Every node calculate $\text{floor}(N/N_{node})$ force vector, except the "master" node, which calculates $\text{floor}(N/N_{node}) + \text{mod}(N, N_{node})$. If CPUs are used for the force calculation, this is the last level of parallelization. The third level is done on GPUs, and it is implemented with CUDA³. If the third level is used, then in every node only N_{GPU} OpenMP thread starts, where N_{GPU} is the number of CUDA-capable GPUs per node. In this case, every second-level thread is used to manage the corresponding GPU in the node: they copy the particle data to the GPU, wait for the end of the force calculation, and copy the calculated forces into the node's shared memory.

We tested the effectiveness of this parallelization with a non-periodic comoving cosmological simulation in the MARCC⁴. We used a standard Λ CDM simulation with $7.6 \cdot 10^6$ dark matter particles for the test. This simulation was run multiple times with different number of GPUs, but we have done only 10 time steps. We averaged the wall-clock time for one simulation time step for every simulation. The calculated speed-up as a function of the number of the GPUs can be seen in fig. 2. We used up to 40 Nvidia Tesla K80 GPUs, and the effectiveness was over 93% for 32 GPUs with 8 MPI tasks.

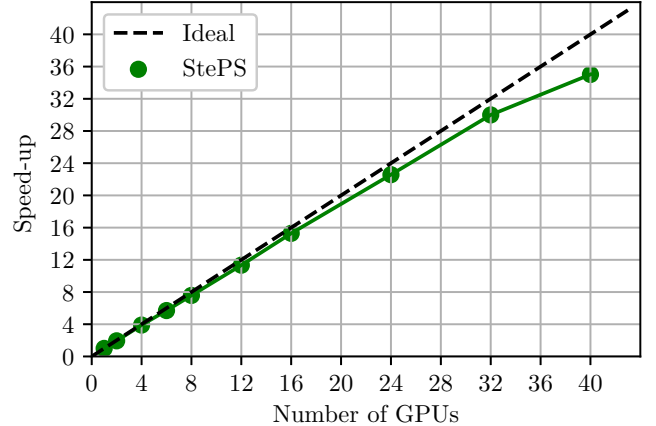


Figure 2: The effectiveness of parallelization of the **StePS** code. See text for discussion.

N_{GPU}	$T_{timestep}(s)$	Number of MPI tasks	Effectiveness
1	5942.11	1	1.0
2	3060.33	1	0.97083
4	1524.02	1	0.97474
6	1042.30	2	0.95016
8	784.11	2	0.94727
12	524.20	3	0.94463
16	388.65	4	0.95557
24	263.21	6	0.94065
32	198.10	8	0.93736
40	169.67	10	0.87554

Table 1: Data from the OpenMP-MPI-CUDA hybrid parallelization test. See text for discussion.

3. Generating Initial Conditions

The main motivation for running cosmological simulations is to calculate the statistical properties of the density field at the present time. To do this, we need to start the simulation from an initial particle distribution from an earlier time with correct statistics. The statistics of the density field from the epoch of the recombination ($z \simeq 1100$) is known from the cosmic microwave background measurements^[9, 10]. From this point, the $P(k)$ power spectrum can be calculated for later times with perturbation theory. These methods are not or not fully taking into account the nonlinear effects, so using these can lead to significant errors in $P(k)$ at high k modes, if the redshift is not high enough. The perturbative methods alone are not suitable to calculate the present $P(k)$ for small scales, but they can be used to generate initial conditions (ICs) for cosmological simulations. In this section we present a new IC generation algorithm for StePS simulations.

3.1. Generating spherical glasses

The first step for generating initial conditions is to generate a particle distribution that represents a uniform density field. This is not an easy problem and it is not clear that a correct

¹<https://www.open-mpi.org/>

²<https://www.openmp.org/>

³<https://developer.nvidia.com/cuda-zone>

⁴<https://www.marcc.jhu.edu/>

answer even exists[11, 12]. Nevertheless, two different solutions are used in the constant resolution periodic case for this problem. The first is the one that places the particles onto a three-dimensional grid. The other solution is using periodic glasses. These methods were suggested by White[13], and they are used in the most of the cosmological N-body simulations nowadays. Particle distribution is made by placing point masses randomly in the periodic box, and evolving them in an Einstein-de Sitter universe with reversed gravity. The simulations with glassy initial conditions show smaller discreteness artifacts at small scales compared to grid-based ICs. The other advantage of this approach is that the glasses are more isotropic.

Our **StePS** code is able to generate glass-like particle distributions in periodic box, but also in our isotropic and non periodic geometry. For generating glasses, the code read an initial particle distribution from an input file and integrates the equations of motions with repulsive gravity and with a chosen boundary condition, just as any other cosmological code. For spherical glasses with decreasing resolution in radial direction, the code needs a special initial condition. We implemented two methods for generating initial conditions for glass making. The first method is called "constant ω binning" method. In this case, we have divided the simulation volume into two distinct regions: to an inner region with constant resolution in real space around the tangent point with r_c radius, and to an outer region with constant resolution in the ω compact coordinate. We divided the compact space into a regularly spaced spherical shells in the outer region. In every shell we place N_{shell} particle randomly, and transform their coordinates into the real space with eq. 2 stereographic projection. The masses of the particles in the shell with index j are

$$m_j = \rho_{\text{crit}} \cdot \Omega_m \cdot \frac{V_{\text{shell},j}}{N_{\text{shell}}}, \quad (19)$$

where $V_{\text{shell},j}$ is the real-space volume of the shell. In the inner spherical region N_{inner} particles are placed randomly with the same mass as the most inner shell in the outer region, where

$$N_{\text{inner}} = \text{floor} \left(\frac{4\pi}{3} r_c^3 \Omega_m \rho_{\text{crit}} / m_{\text{inner}} \right). \quad (20)$$

The division of the simulation volume into this two distinct regions is necessary, since with this constant ω binning the resolution is increasing too fast in inward direction after a certain point, and the mixing of the particles with too large mass differences can cause artificial distortions in the simulations. The main advantage of this method is that if one chooses large enough inner volume, the effect of the mixing particles will be minimal at the center. We used similar compactification in our previous paper.

The other implemented binning method is the "constant compact space volume" method. In this case the script uses an ω dependent shell thickness where the shells in the compact space have equal volume. The equation for the lower limit of the i -th shell in the ω coordinate is:

$$\frac{8V_{\text{bin}}^{\text{comp}}}{\pi D_s^3} \cdot i = 2\omega_i^l - \sin(2\omega_i^l), \quad (21)$$

where $V_{\text{bin}}^{\text{comp}}$ is the volume of a bin in the compact space. This equation must be solved numerically for each i shell. After the limits for the shells are calculated, we place N_{shell} particle randomly into this compact shell, and transform back to the real space. The particle masses calculated from eq. 19 for every shell. With this method the particle masses will decrease smoothly outwards for the whole simulation volume.

Many other realizations are possible: one can use different compactification maps, or it is possible to change the angular resolution by setting N_{shell} to ω dependent, etc. We will discuss these possibilities in a future study.

With the generated initial condition, and the integration of the eq. 10 with reversed gravity, after a long relaxation period the particles settle down to a glass-like configuration. This three-dimensional spherical glass with changing resolution in radial direction can be used for generating initial conditions.

3.2. Perturbing the glass particles

Our simulation code alone does not generate initial conditions from glass. For this, we wrote a separate script in python, and made it freely available. Below we summarize the basic ideas of the generation of initial conditions for periodic simulations, and after that we describe our new algorithm for the **StePS** geometry.

After a particle distribution that represents a homogeneous universe is available in a constant resolution periodic box, the next step is to calculate the power spectrum for the initial time snapshot. In linear Eulerian perturbation theory, every k mode of the $P(k)$ power spectrum are evolving independently, and they can be scaled to any scalefactor via the

$$D(a) = \frac{5\Omega_m H_0}{2} H(a) \int_0^a \frac{da'}{a'^3} \quad (22)$$

growth function[14]. The power spectrum should be normalized at present day scalefactor to be consistent with the σ_8 cosmological parameter. After the initial power spectrum calculated, the $\delta(\mathbf{k})$ Fourier transform of the density fluctuation field can be generated assuming Gaussian random field[12]. $\delta(\mathbf{k})$ is calculated in a finite range: from zero to the $k_{Ny} = \pi/\Delta x$ Nyquist wavenumber in each dimension, which is given by the average particle spacing.

If the density field is calculated, we only need to perturb the positions and speeds of the particles, to generate the initial condition. In the Lagrangian fluid dynamics, the movement of a fluid elements is described by its $x(t_0)$ initial coordinate and the displacement field $\Psi(x(t_0), t)$,

$$x(t) = x(t_0) + \Psi(x(t_0), t) \quad (23)$$

where t_0 is the initial time, and $\Psi(x(t_0), t_0) = 0$. The Lagrangian Perturbation Theory (LPT) uses a perturbative solution for the calculation of the displacement field from the Fourier-space density fluctuations[15, 16],

$$\Psi(x(t_0), t) = \Psi^{(1)}(x(t_0), t) + \Psi^{(2)}(x(t_0), t) + \Psi^{(3)}(x(t_0), t) + \dots \quad (24)$$

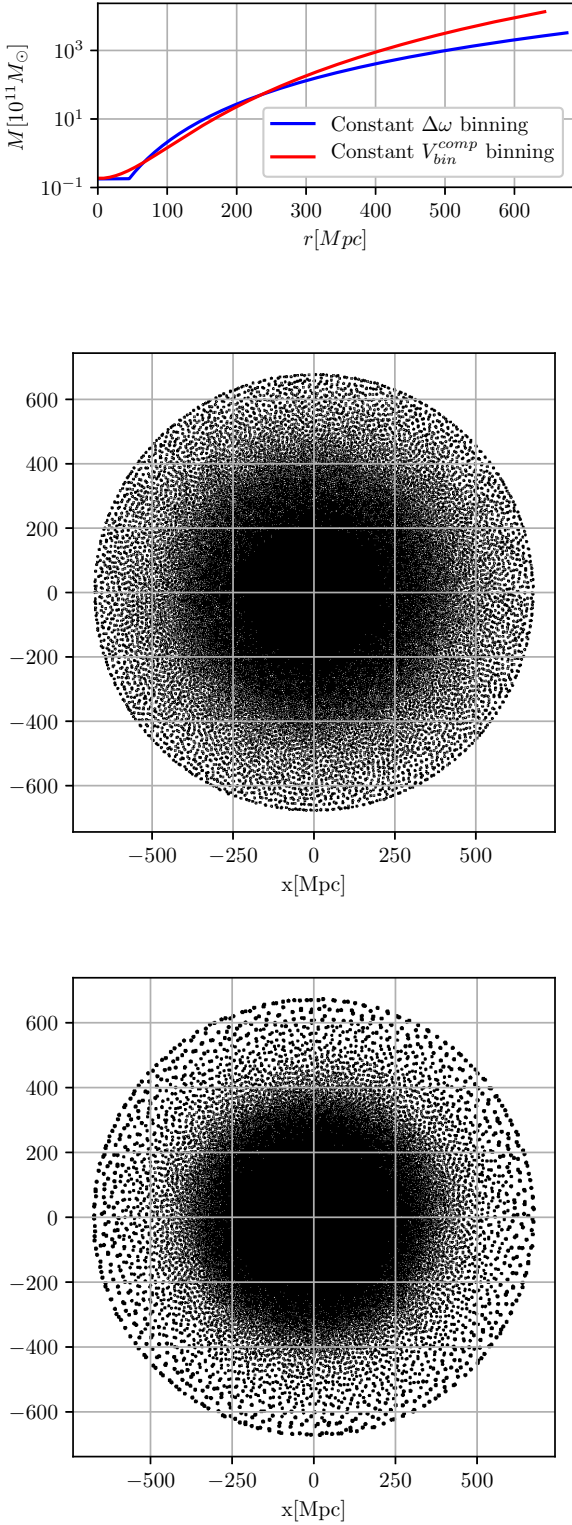


Figure 3: The generated example spherical glasses. **Top:** Mass resolution as a function of radius in two example spherical glass with different binning method. The parameters of the constant $\Delta\omega$ glass were the following: $D_s = 60.0 \text{ Mpc}$, $r_c = 45.0 \text{ Mpc}$, $D_{\text{sim}} = 684.9 \text{ Mpc}$, $N_{\text{radial}} = 600$, $N_{\text{shell}} = 12288$. The constant $V_{text{bin}}^{comp}$ glass had the wollowing parameters: $D_s = 100.0 \text{ Mpc}$, $D_{\text{sim}} = 684.9 \text{ Mpc}$, $N_{\text{radial}} = 405$, $N_{\text{shell}} = 12288$. We used an EdS Universe for background through the glass making. **Center and Bottom:** A 4 degree thick slices from the glasses generated with constant $\Delta\omega$ and constant $V_{text{bin}}^{comp}$ binning method respectively. The plotted size of the particles are proportional with their masses. The total number of the particles were $N = 4.9 \cdot 10^6$ in both cases.

the first order solution is the Zel'dovich-approximation[17], which can be written as

$$\Psi^{(1)}(\mathbf{q}) = \int \frac{i\mathbf{k}}{k^2} \delta(\mathbf{k}) e^{i\mathbf{q}\mathbf{k}} \quad (25)$$

$$\mathbf{x} = q + \Psi^{(1)}(\mathbf{q}) \quad (26)$$

$$\dot{\mathbf{x}} = \frac{\dot{D}(a)}{D(1)} \Psi(\mathbf{q}), \quad (27)$$

where \mathbf{q} are the initial, and \mathbf{x} are the final coordinates of the particles. Of course the $\Psi(q)$ displacement field is calculated in a cubic grid, and got interpolated to the glass particles original position. Similarly, the second order solution of the Lagrange perturbation theory (2LPT)[18] also used for initial condition generation. After the positions of the particles are set, the last step is to set their masses with eq. 8.

The IC generation algorithm for our spherically symmetric geometry is very similar, but there are two main differences. The first is that we do not have a constant average particle spacing for our simulation volume, because the mass and the spatial resolution is decreasing in radial direction. The second difference is that we do not have a periodic geometry, so we can freely choose the real-space box-size for the density fluctuation field that will be used in the Zel'dovich approximation. This two differences raise a question: how do we choose the limits of the $\delta(\mathbf{k})$ fluctuation field in the \mathbf{k} space?

The lower, non-zero \mathbf{k} determines the real space box size of the periodic density field. If interested in the effects of the periodicity, one should choose $L_{\text{box}}/2 < R_{\text{sim}}$. In this case, the same density field will be repeated multiple times over the non-periodic IC. If one chooses $L_{\text{box}}/2 > R_{\text{sim}}$, then only a smaller part of the periodic volume will be used, and with this one can efficiently model the super-survey modes and the cosmic variances.

The larger k in every axis determines the real space resolution. We implemented two methods for calculating the displacement field: the simplest is using the $\pi/\Delta x_{inner}$ Nyquist wavenumber that corresponds to the best resolution inner part of the simulation. In this case only one displacement field is calculated, and the particles are perturbed with the eq. 27 Zel'dovich or with the 2LPT method. With this method, it is possible to do an "oversample" if the dynamic range is large enough. In this case if one uses too large resolution fluctuation field in a low resolution region, the displacement of the particles that represent a larger part of the field will include the smaller scale perturbations that are not resolved in that scale. The second implemented method is free from this oversampling: in this, the script calculates multiple displacement fields with different k_{Ny} Nyquist frequency, and interpolating between these due the radius dependent $\Delta x(r)$ average displacement and use this field for the perturbation. For the calculation of the displacement fields, our script in both cases use the publicly available **Ngenic**[19] and **2LPTic**[20] codes for the Zel'dovich and the 2LPT approximations respectively.

The next step is to set the particle masses to be consistent with the desired cosmological parameters. This can be easily

done by setting

$$m_j = m_j^{\text{glass}} \frac{\Omega_m \rho_{\text{crit}} \cdot \frac{4\pi}{3} R_{\text{sim}}^3}{\sum_{i=1}^N m_i^{\text{glass}}}, \quad (28)$$

where m_j is the mass of the j th particle, m_j^{glass} is the original mass of the glass particle, and R_{sim} is the radius of the simulation. If the goal is to generate an IC for non-comoving simulation, then one last step should be done: the rescaling the coordinates and speeds with eq. 12. After this point the script writes out the initial condition into a predetermined file.

4. Example simulation

For demonstration, we aimed to re-simulate the Millennium Run[21] with the **StePS** code. The Millennium simulation had a great impact and demonstrated the effectiveness of the GADGET-2 cosmological tree code. The original simulation used 2160^3 particles in a periodic cube with 684.9Mpc length. It used 512 processors and required about 28 days of wall-clock time on an IBM p690 supercomputer. We used the same parameters and random seed for generating the initial condition for our non-periodic StePS simulation. The R_{sim} simulation was 684.9Mpc, and we used constant ω binning. The diameter of the constant high resolution sphere inside the simulation volume was 90Mpc. The spatial resolution at the center was ~ 1.6 times worse than the original Millennium simulation. The parameters of both simulations can be seen in table 2.

	Millennium	StePS
Ω_m	0.25	
Ω_Λ	0.75	
H_0 [km/s/Mpc]	73.0	
σ_8	0.9	
Initial redshift	127	
linear size [Mpc]	$L_{\text{box}} = 684.9$	$R_{\text{sim}} = 684.9$
simulated volume [Gpc 3]	0.321	1.35
number of particles	1.01×10^{10}	1.17×10^7
particle mass [M_\odot]	1.2×10^9	$5.2 \times 10^9\text{--}10^{14}$
force calculation	$\mathcal{O}(N \log N)$	$\mathcal{O}(N^2)$
memory use [GB]	$\sim 1,000$	0.342
number of processing units	512 (CPU)	12 (GPU)
wall-clock time [h]	683	106

Table 2: Main parameters of the compared simulations.

4.1. Results

Our simulation used 12 Nvidia GeForce 1080ti GPUs, and it took 106 wall-clock hours. For the easier comparison we made a compactified version of the $z = 0$ Millennium snapshot. We did this by placing multiple copies periodically of the original $z = 0$ snapshot, and transformed it into the compact space by using eq. 1. We binned the particle data with constant ω binning in radial direction and equal-area HEALPix[22] tiling in the ϑ and φ coordinates. We averaged the positions, summed up the

masses and inertia of the dark matter particles in each bin to replace them with one particle. After this point, we simply decompactified the newly generated particles with eq. 2. As a result, we got a particle distribution which has nearly identical resolution-radius function as our own simulation. The comparison of Millennium and our **StePS** simulation in different scales can be seen in fig. 4.

5. Summary

We presented a multi-GPU implementation of the **StePS** code, and demonstrated the effectiveness of the parallelization. We also implemented a new initial condition generator script for compactified simulations. We were able to reconstruct the Millennium simulation with ~ 1.6 times less resolution in the center with our codes, under 106 hours. The source code of the simulation program and the IC generator script is freely available at our github repository (<https://github.com/elitevo/StePS>), and it licensed under GNU General Public License v2.0.

Acknowledgements

The authors would like to thank Volker Springel and Adrian Jenkins for helping recreate the Millennium initial conditions. We also want to thank Robert Beck for stimulating discussions. This work has been supported by the NKFI grants NN 114560 and NN 129148. IS acknowledges support from National Science Foundation (NSF) award 1616974. We would like to thank the GPU Laboratory of Hungarian Academy of Sciences Wigner Research Centre of Physics for providing computing resources. Part of this research project was conducted using computational resources at the Maryland Advanced Research Computing Center (MARCC).

References

- [1] W. H. Press, P. Schechter, Formation of Galaxies and Clusters of Galaxies by Self-Similar Gravitational Condensation, *ApJ*187 (1974) 425–438. [doi:10.1086/152650](https://doi.org/10.1086/152650).
- [2] D. Potter, J. Stadel, R. Teyssier, PKDGRAV3: beyond trillion particle cosmological simulations for the next era of galaxy surveys, *Computational Astrophysics and Cosmology* 4 (2017) 2. [arXiv:1609.08621](https://arxiv.org/abs/1609.08621), [doi:10.1186/s40668-017-0021-1](https://doi.org/10.1186/s40668-017-0021-1).
- [3] G. Rácz, I. Szapudi, I. Csabai, L. Dobos, Compactified cosmological simulations of the infinite universe, *MNRAS*477 (2018) 1949–1957. [arXiv:1711.04959](https://arxiv.org/abs/1711.04959), [doi:10.1093/mnras/sty695](https://doi.org/10.1093/mnras/sty695).
- [4] V. Springel, The cosmological simulation code GADGET-2, *MNRAS*364 (2005) 1105–1134. [arXiv:astro-ph/0505010](https://arxiv.org/abs/astro-ph/0505010), [doi:10.1111/j.1365-2966.2005.09655.x](https://doi.org/10.1111/j.1365-2966.2005.09655.x).
- [5] J. J. Monaghan, J. C. Lattanzio, A refined particle method for astrophysical problems, *A&A*149 (1985) 135–143.

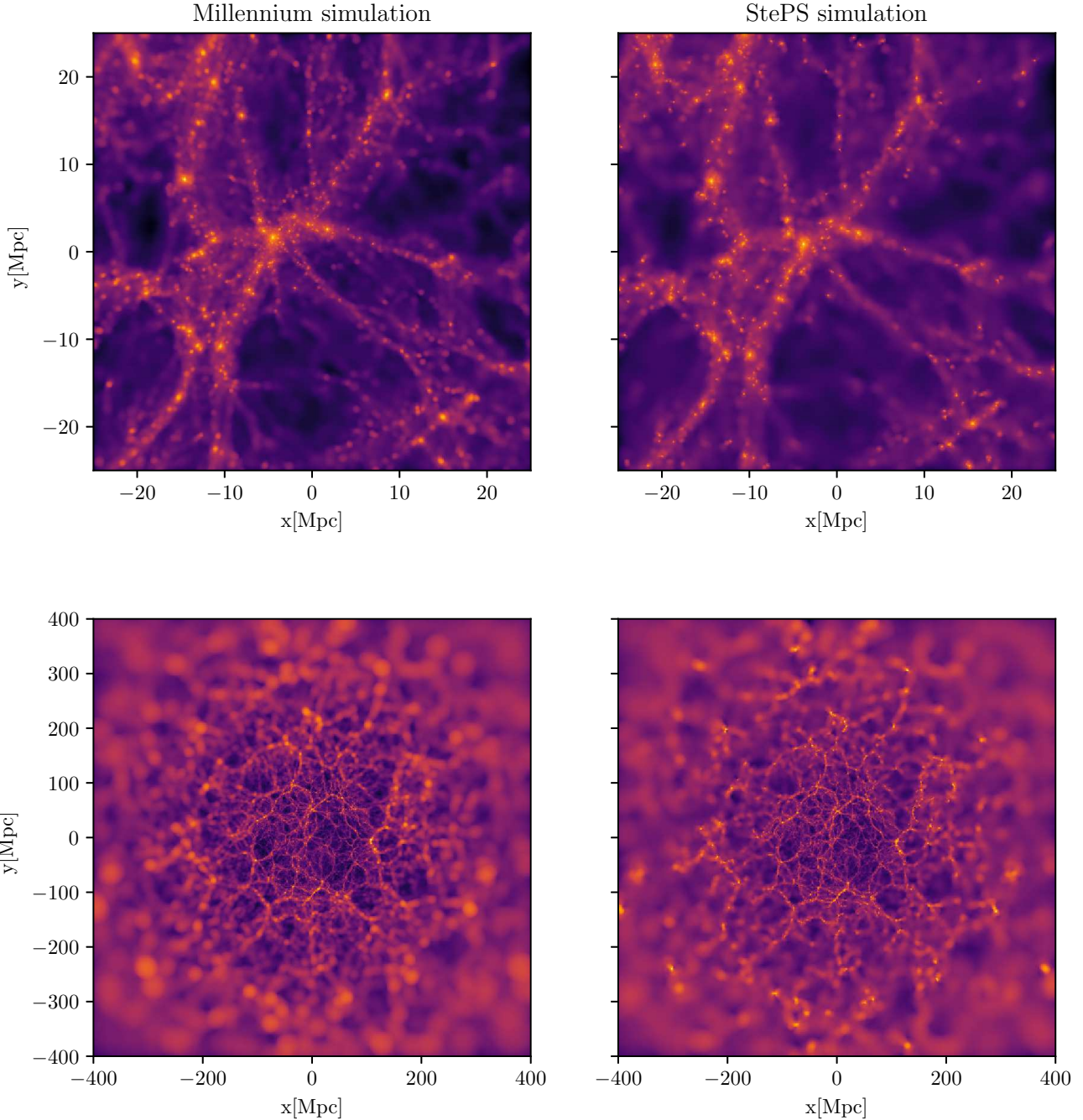


Figure 4: Visualization of distribution of the dark matter in the Millennium and in our **StePS** simulation at $z = 0$, in different scales. For the easier comparison we used a compactified version of the Millennium snapshot. The thickness of the density slices were 10Mpc . See text for details.

[6] P. P. Ewald, Die Berechnung optischer und elektrostatischer Gitterpotentiale, *Annalen der Physik* 369 (1921) 253–287. [doi:10.1002/andp.19213690304](https://doi.org/10.1002/andp.19213690304).

[7] L. Hernquist, F. R. Bouchet, Y. Suto, Application of the Ewald method to cosmological N-body simulations, *ApJS75* (1991) 231–240. [doi:10.1086/191530](https://doi.org/10.1086/191530).

[8] T. Quinn, N. Katz, J. Stadel, G. Lake, Time stepping N-body simulations, *ArXiv Astrophysics e-prints* [arXiv:astro-ph/9710043](https://arxiv.org/abs/astro-ph/9710043).

[9] C. L. Bennett, D. Larson, J. L. Weiland, N. Jarosik, G. Hinshaw, N. Odegard, K. M. Smith, R. S. Hill, B. Gold, M. Halpern, E. Komatsu, M. R. Nolta, L. Page, D. N. Spergel, E. Wollack, J. Dunkley, A. Kogut, M. Limon, S. S. Meyer, G. S. Tucker, E. L. Wright, Nine-year Wilkinson Microwave Anisotropy Probe (WMAP) Observations: Final Maps and Results, *ApJS208* (2013) 20. [arXiv:1212.5225](https://arxiv.org/abs/1212.5225), [doi:10.1088/0067-0049/208/2/20](https://doi.org/10.1088/0067-0049/208/2/20).

[10] Planck Collaboration, N. Aghanim, Y. Akrami, M. Ashdown, J. Aumont, C. Baccigalupi, M. Ballardini, A. J. Banday, R. B. Barreiro, N. Bartolo, S. Basak, R. Battye, K. Benabed, J.-P. Bernard, M. Bersanelli, P. Bielewicz, J. J. Bock, J. R. Bond, J. Borrill, F. R. Bouchet, F. Boulanger, M. Bucher, C. Burigana, R. C. Butler, E. Calabrese, J.-F. Cardoso, J. Carron, A. Challinor, H. C. Chiang, J. Chluba, L. P. L. Colombo, C. Combet, D. Contreras, B. P. Crill, F. Cuttaia, P. de Bernardis, G. de Zotti, J. Delabrouille, J.-M. Delouis, E. Di Valentino, J. M. Diego, O. Doré, M. Douspis, A. Ducout, X. Dupac, S. Dusini, G. Efstathiou, F. Elsner, T. A. Enßlin, H. K. Eriksen, Y. Fantaye, M. Farhang, J. Fergusson, R. Fernandez-Cobos, F. Finelli, F. Forastieri, M. Frailis, E. Franceschi, A. Frolov, S. Galeotta, S. Galli, K. Ganga, R. T. Génova-Santos, M. Gerbino, T. Ghosh, J. González-Nuevo, K. M. Górski, S. Gratton, A. Gruppuso, J. E. Gudmundsson, J. Hamann, W. Handley, D. Herranz, E. Hivon, Z. Huang, A. H. Jaffe, W. C. Jones, A. Karakci, E. Keihänen, R. Keskitalo, K. Kiiveri, J. Kim, T. S. Kisner, L. Knox, N. Krachmalnicoff, M. Kunz, H. Kurki-Suonio, G. Lagache, J.-M. Lamarre, A. Lasenby, M. Lattanzi, C. R. Lawrence, M. Le Jeune, P. Lemos, J. Lesgourges, F. Levrier, A. Lewis, M. Liguori, P. B. Lilje, M. Lilley, V. Lindholm, M. López-Caniego, P. M. Lubin, Y.-Z. Ma, J. F. Macías-Pérez, G. Maggio, D. Maino, N. Mandolcsi, A. Mangilli, A. Marcos-Caballero, M. Maris, P. G. Martin, M. Martinelli, E. Martínez-González, S. Matarrese, N. Mauri, J. D. McEwen, P. R. Meinhold, A. Melchiorri, A. Mennella, M. Migliaccio, M. Millea, S. Mitra, M.-A. Miville-Deschénes, D. Molinari, L. Montier, G. Morgante, A. Moss, P. Natoli, H. U. Nørgaard-Nielsen, L. Pagano, D. Paoletti, B. Partridge, G. Patanchon, H. V. Peiris, F. Perrotta, V. Pettorino, F. Piacentini, L. Polastri, G. Polenta, J.-L. Puget, J. P. Rachen, M. Reinecke, M. Rezaie, A. Renzi, G. Rocha, C. Rosset, G. Roudier, J. A. Rubiño-Martín, B. Ruiz-Granados, L. Salvati, M. Sandri, M. Savelainen, D. Scott, E. P. S. Shellard, C. Sirignano, G. Sirri, L. D. Spencer, R. Sunyaev, A.-S. Suur-Uski, J. A. Tauber, D. Tavagnacco, M. Tenti, L. Toffolatti, M. Tomasi, T. Trombetti, L. Valenziano, J. Valiviita, B. Van Tent, L. Vibert, P. Vielva, F. Villa, N. Vittorio, B. D. Wandelt, I. K. Wehus, M. White, S. D. M. White, A. Zacchei, A. Zonca, Planck 2018 results. VI. Cosmological parameters, *ArXiv e-prints* [arXiv:1807.06209](https://arxiv.org/abs/1807.06209).

[11] L. Hernquist, N. Katz, TREESPH - A unification of SPH with the hierarchical tree method, *ApJS70* (1989) 419–446. [doi:10.1086/191344](https://doi.org/10.1086/191344).

[12] E. Sirkо, Initial Conditions to Cosmological N-Body Simulations, or, How to Run an Ensemble of Simulations, *ApJ634* (2005) 728–743. [arXiv:astro-ph/0503106](https://arxiv.org/abs/astro-ph/0503106), [doi:10.1086/497090](https://doi.org/10.1086/497090).

[13] S. D. M. White, Formation and Evolution of Galaxies: Les Houches Lectures, *ArXiv Astrophysics e-prints* [arXiv:astro-ph/9410043](https://arxiv.org/abs/astro-ph/9410043).

[14] S. Dodelson, *Modern cosmology*, Academic Press, 2003.

[15] I. B. Zeldovich, The theory of the large scale structure of the universe, in: M. S. Longair, J. Einasto (Eds.), *Large Scale Structures in the Universe*, Vol. 79 of IAU Symposium, 1978, pp. 409–420.

[16] M. White, The Zel'dovich approximation, *MNRAS439* (2014) 3630–3640. [arXiv:1401.5466](https://arxiv.org/abs/1401.5466), [doi:10.1093/mnras/stu209](https://doi.org/10.1093/mnras/stu209).

[17] Y. B. Zel'dovich, Gravitational instability: An approximate theory for large density perturbations., *A&A5* (1970) 84–89.

[18] M. Crocce, S. Pueblas, R. Scoccimarro, Transients from initial conditions in cosmological simulations, *MNRAS373* (2006) 369–381. [arXiv:astro-ph/0606505](https://arxiv.org/abs/astro-ph/0606505), [doi:10.1111/j.1365-2966.2006.11040.x](https://doi.org/10.1111/j.1365-2966.2006.11040.x).

[19] V. Springel, NGenIC: Cosmological structure initial conditions, *Astrophysics Source Code Library* (Feb. 2015). [arXiv:1502.003](https://arxiv.org/abs/1502.003).

[20] M. Crocce, S. Pueblas, R. Scoccimarro, 2LPTIC: 2nd-order Lagrangian Perturbation Theory Initial Conditions, *Astrophysics Source Code Library* (Jan. 2012). [arXiv:1201.005](https://arxiv.org/abs/1201.005).

[21] V. Springel, S. D. M. White, A. Jenkins, C. S. Frenk, N. Yoshida, L. Gao, J. Navarro, R. Thacker, D. Croton, J. Helly, J. A. Peacock, S. Cole, P. Thomas, H. Couchman, A. Evrard, J. Colberg, F. Pearce, Simulations of the formation, evolution and clustering of galaxies and quasars, *Nature435* (2005) 629–636. [arXiv:astro-ph/0504097](https://arxiv.org/abs/astro-ph/0504097), [doi:10.1038/nature03597](https://doi.org/10.1038/nature03597).

[22] K. M. Górski, E. Hivon, A. J. Banday, B. D. Wandelt, F. K. Hansen, M. Reinecke, M. Bartelmann, HEALPix: A Framework for High-Resolution Discretization and Fast Analysis of Data Distributed on the Sphere, *ApJ622* (2005) 759–771. [arXiv:astro-ph/0409513](https://arxiv.org/abs/astro-ph/0409513), [doi:10.1086/427976](https://doi.org/10.1086/427976).